

Narrowband Excitation of ^2H Powder Pattern and Its Application to ^2H 1D Exchange Sample-Turning NMR

D. Reichert,¹ Takashi Mizuno, K. Takegoshi, and Takehiko Terao²

Department of Chemistry, Graduate School of Science, Kyoto University, Kyoto 606-8502, Japan

Received December 7, 1998; revised April 20, 1999

Frequency-selective narrowband excitation of the ^2H powder pattern was examined. Selection of a single spectral band with a linewidth of ca. 15 kHz was achieved by a narrowband $^1\text{H} \rightarrow ^2\text{H}$ cross polarization by using the time-averaged precession frequency method. Further narrowing with a ca. 5 kHz linewidth is achieved by DANTE irradiation. The narrowband excitation was applied to transform a recently developed 2D spin-exchange method for obtaining structural information (*Chem. Phys. Lett.* **260, 159, (1996)) into its 1D analogue. The determination of the D–C–D bond angle was demonstrated for α -glycine-[2,2- d_2]. Further, the intermolecular polarization transfer between two deuterons separated by 0.299 nm was detected with the mixing time of 500 μs .**

© 1999 Academic Press

Key Words: narrowband excitation; solid-state NMR; spin exchange; deuterium; molecular structure.

INTRODUCTION

Since a deuteron (^2H) quadrupolar interaction has a well-defined orientation in the molecular frame, ^2H NMR has been a powerful method for investigating molecular motion (1). In particular, Spiess and co-workers have shown that, applying two-dimensional (2D) exchange NMR, one can very precisely obtain information about a dynamical process such as jump angles and site populations (2). Recently, we showed that the same deuteron 2D exchange NMR scheme allows us to determine the relative orientation of two different C–D bonds in rigid lattice. In this case, however, the two ^2H quadrupolar interactions are correlated by polarization transfer instead of molecular motion (3). Polarization transfer between two ^2H spins is exceedingly slow and orientation-dependent because of the large anisotropic quadrupolar interactions. The transfer efficiency was dramatically improved by implementing mechanical sample turning during the mixing time, which provides dynamical matching of the orientation-dependent quadrupolar frequencies of different spins. The precise

determination of the interbond angle in α -glycine-[2,2- d_2] was successfully demonstrated (3).

Selective excitation in multidimensional experiments is generally incorporated to reduce the experimental time and the dimensionality required to unravel overlapping signals. Here, we present a 1D version of the 2D exchange sample-turning experiment owing to the following reason. In the 2D experiment, a quadrature detection was not done in the t_1 domain because the quadrupolar order cannot survive through the mixing period (3). This leads to aliasing of huge diagonal signals, which makes it difficult to resolve cross peaks around the aliased diagonal lines. It may be envisaged that the aliasing problem can be avoided by switching to 1D exchange methods, rather than performing 2D experiments. In this work, a narrow frequency band of the ^2H powder pattern, representing a selected orientation of C–D bonds, is excited to obtain the 1D exchange spectrum, which is equal to the cross section of the 2D spectrum at the excited (initial) frequency. It should be mentioned that this scheme is similar to the ^{13}C 1D exchange experiment (4) and the “hole-burning” experiment (5), which were used to detect slow molecular motions in solids.

Selective excitation or saturation of a desired region of the spectrum can be performed using a soft 90° pulse, a shaped pulse (6), the DANTE pulse train (7), or the SELDOM sequence (8). In the present experiment, a narrowband $^1\text{H} \rightarrow ^2\text{H}$ cross polarization (CP) based on the TAPF sequence (9), which effectively reduces the RF intensity for ^2H required for CP, was used to take advantage of the much shorter T_1 of ^1H than that of ^2H and of the gain in sensitivity. Further narrowing was achieved by the DANTE sequence. We will describe the details and report the experimental results for α -glycine-[2,2- d_2] (glycine- d_2).

Following the 2D exchange sample-turning experiment, Gan *et al.* reported a similar 2D experiment using slow magic-angle sample spinning instead of sample turning (10). The latter approach requires precise synchronization of RF pulses with sample spinning, although a commonly available probe can be used. The efficiency of the RF irradiation as well as the signal-to-noise ratio is better for the 90° -oriented sample-coil for the sample-turning experiment than the magic-angle-oriented coil for their scheme. Furthermore, it is worthy to point

¹ Present address: Halle University, Department of Physics, Friedemann-Bach-Platz 6, 06108 Halle, Germany.

² To whom correspondence should be addressed. E-mail: terao@kuchem.kyoto-u.ac.jp.

out that it is difficult to incorporate the present narrowband excitation method into the slow magic-angle sample spinning experiment.

EXPERIMENTAL

α -Glycine-[2,2- d_2] was purchased from Cambridge Isotope Labs. and used without further purification. The NMR experiments were performed using a Chemagnetics CMX-300 spectrometer operating at 46 MHz for ^2H utilizing a homebuilt double-tuned sample-turning probe (3). In this probe, a sample tube with an outer diameter of 6.5 mm can be turned by a stepping motor around an axis perpendicular to the static magnetic field direction. A typical 90° pulse length for deuterons was 2 μs .

RESULTS AND DISCUSSION

Narrowband Excitation of a ^2H Powder Pattern

In the 2D ^2H exchange sample-turning experiment (3), CP from ^1H to ^2H rather than direct ^2H excitation by a $\pi/2$ -pulse was applied to circumvent the very long ^2H T_1 in rigid lattice and to make use of the signal enhancement due to CP. However, owing to the large spectral width of a ^2H powder pattern with the spectral width of about 250 kHz (Fig. 1a), only a part of it can be polarized by the protons, depending on the ratio $\nu_{2\text{H}}/\nu_{1\text{H}}$ (see Fig. 1 of Ref. (3)). While this distortion was removed by adiabatically increased $\nu_{2\text{H}}$ under a constant $\nu_{1\text{H}}$ in the 2D experiment, in the present case we take advantage of the narrowband cross polarizations. We applied a constant amplitude single-quantum CP with $\nu_{2\text{H}} = \nu_{1\text{H}} = 63$ kHz, and by doing so, we could reduce the broad ^2H spectrum to a single line with a width of ca. 32 kHz, which is centered at the on-resonance frequency (Fig. 1b). It is also possible to excite signals at off-resonance frequencies by applying off-Hartman–Hahn conditions $\nu_{2\text{H}} \neq \nu_{1\text{H}}$ (Fig. 1 of Ref. (3)). In this work, we used the Hartman–Hahn condition $\nu_{2\text{H}} = \nu_{1\text{H}}$ and chose the on-resonance frequency at the center of the powder pattern. Since the signals near the center of the powder pattern come from the spins whose quadrupolar interactions are small, their response to RF irradiation can be calculated easily.

Reduction of the ^2H RF field intensity in CP would result in the narrowing of the width of the excited line. To maintain the Hartmann–Hahn condition $\nu_{2\text{H}} = \nu_{1\text{H}}$, one needs to decrease the intensity of the ^1H RF field, too. However, simple reduction of $\nu_{1\text{H}}$ diminishes the coherence to a large extent when $\nu_{1\text{H}}$ is comparable to or weaker than the local field. To solve this dilemma, we applied the method of “time-averaged precession frequency” (TAPF) which allows us to fulfill the Hartman–Hahn condition with low $\nu_{2\text{H}}$ while we keep $\nu_{1\text{H}}$ at a high level: TAPF effectively reduces $\nu_{1\text{H}}$ by alternating the phase of the ^1H RF field between 0 and π with different duration times (9). We have chosen the time intervals of the phase alternation of the

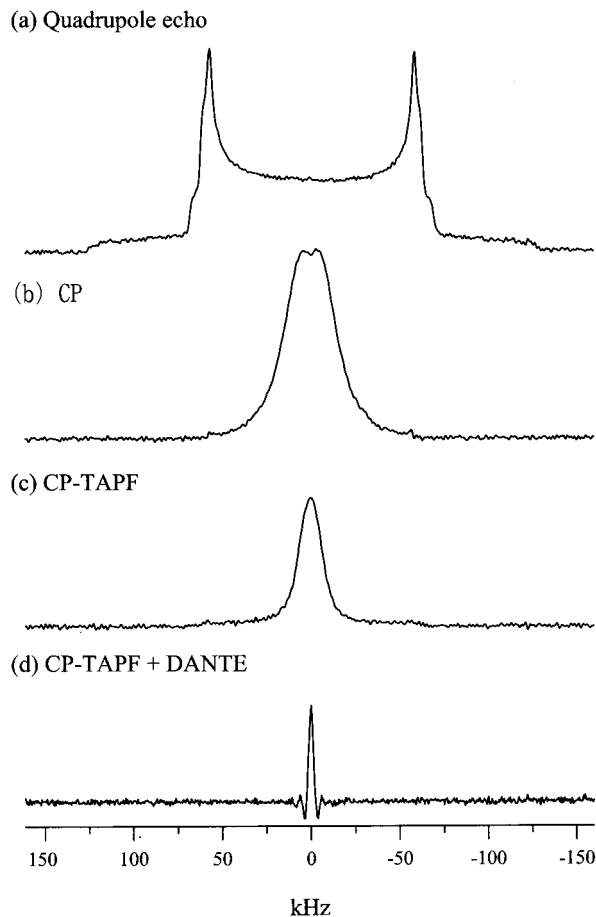


FIG. 1. Steps toward the narrowband excitation of the ^2H powder pattern. Sixty-four accumulations each. ^1H decoupling was applied during signal acquisition in all experiments. (a) Full powder pattern obtained by a quadrupole-echo sequence ($\pi/2$ -pulse width = 2 μs , $\tau = 20$ μs , 300 s repetition time). (b) Selectively excited spectrum obtained by normal single-quantum cross polarization and an appended reading pulse to create a quadrupole echo ($\nu_{2\text{H}} = \nu_{1\text{H}} = 60$ kHz, 7 ms CP contact time, 2 s repetition time). (c) Cross polarization spectrum narrowed by reducing the CP RF field intensities. TAPF (11) was used for effectively reducing the ^1H RF field intensity ($\nu_{2\text{H}} = 0.05\nu_{1\text{H}} = 3$ kHz, 2 s repetition time). (d) Finally narrowed resonance line obtained by (c) +DANTE (20 pulses, 0.1 μs pulse width each, 10 μs delay, 1 s repetition time). ^1H decoupling was applied during the DANTE pulse train.

^1H irradiation to be 3.8 and 4.2 μs . Accordingly, $\nu_{1\text{H}}$ can be effectively reduced by the ratio of $0.4/8 = 0.05$ to match the Hartman–Hahn condition with low $\nu_{2\text{H}}$. This decreases the width of the excited line to about 15 kHz (Fig. 1c). This bandwidth may be narrow enough for many applications. For example, as will be shown in Fig. 4a, a number of singularities can already be resolved in the 1D exchange spectrum. Therefore, for a less demanding experiment, the TAPF selection might be satisfying already.

To reduce the width of the excited line further, we checked two approaches. Firstly, we applied a filter sequence that is based on the SELDOM pulse train (8) with a pulse spacing of τ_1 . In its original version, the spectral intensity of the initial

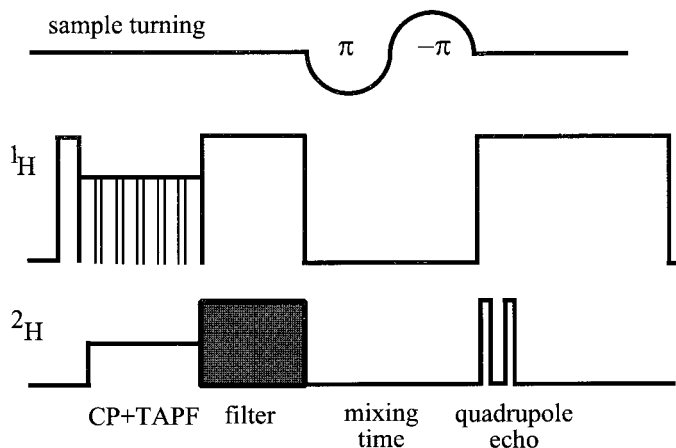


FIG. 2. Experimental sequence of the 1D exchange sample-turning experiment. It utilizes $^1\text{H} \rightarrow ^2\text{H}$ cross polarization with a low ^2H RF field, a filter sequence (either DANTE or “dynamic SELDOM”), sample turning during the mixing time, and the quadrupole echo for detection. The intensity of ^1H RF field for CP is scaled by TAPF (9). ^1H decoupling was applied during both the filter sequence and the acquisition.

magnetization is modulated by $\cos^N(\omega\tau_1)$ after application of N cycles, leading to an effective suppression of all frequencies but those equal to $\omega\tau_1 = K\pi$ ($K = 0, 1, \dots$). To improve the efficiency of the filter, we increased τ_1 after each cycle according to $\tau_1(i+1) = 1.35\tau_1(i)$ (“dynamic SELDOM”). While the former maintains undesirable signals at frequencies $f = n/2\tau$, ($n = 1, 2, \dots$), the latter performs the selection of $f_1 = 0$ only. By starting at $\tau_1 = 25 \mu\text{s}$ and $N = 4$, we achieved the linewidth of ca. 5 kHz. Secondly, we checked the DANTE pulse train (7) as a tool for final narrowing. It barely suffers from signal loss by imperfect pulses. However, the spectrum exhibits “DANTE-wiggles” (7) around the base of the peak, which might obscure possible exchange signals in this spectral region. Since we do not expect any exchange signals there except the singularity close to $f_1 = 0$ (see Fig. 3a), we used the DANTE pulse train rather than the dynamic SELDOM. However, in case one would expect exchange peaks within a range of some ± 10 kHz around the excited line, one should use the latter. We noticed that a combined use of the narrowband cross polarization and the DANTE train works with about 30% loss of spectral intensity at $f_1 = 0$, while SELDOM suffers from a severe loss due to imperfect pulses and relaxation during the pulse train.

1D-Exchange Sample-Turning NMR

The pulse sequence of the 1D exchange experiment (Fig. 2) follows the general structure of a 2D experiment: preparation, evolution, mixing, and detection. In our case, both preparation (creation of transverse magnetization) and evolution (creation of a defined initial condition for the exchange process) serve for the excitation of a selected ensemble of spins resonating at frequency f_1 . This magnetization is brought into longitudinal

magnetization by the following $\pi/2$ pulse. During the mixing time, sample turning causes the exchange of polarizations between neighboring spins. We applied turning by an angle of π , followed immediately by another turning by $-\pi$ back to its original position. After the mixing time, the longitudinal magnetization is turned back into observable magnetization by the second $\pi/2$ pulse to record the signal. The ridges of the 2D spectrum finally appear as peaks in the 1D exchange spectrum after Fourier transformation.

The notable difference of the 1D experiment, compared to the 2D experiment, is the excitation at a single frequency f_1 rather than sampling the complete spectrum by incrementing the evolution delay t_1 . Practically, one can excite not a single frequency but a finite frequency band. This broadens the 1D exchange peaks due to overlap of the ridges belonging to this band of excited frequencies. Figure 3a shows the ridge plot for polarization transfer between the deuterons D(4) and D(5) of

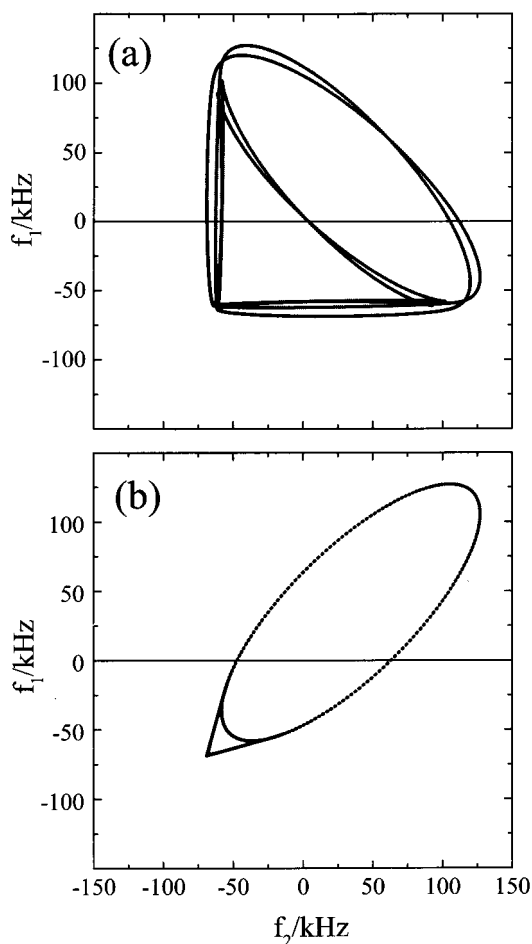


FIG. 3. Theoretical 2D ridge plots. (a) Plot due to spin diffusion between the two deuterons within the same glycine- d_2 molecule. The tensor parameters used for the simulation are given in Table 1. (b) Plot due to spin diffusion between the third-nearest pair of D(4) deuterons in a unit cell of glycine- d_2 . The angles relating the two principal axis system are ($\phi = 0^\circ$, $\theta = 159.4^\circ$, $\chi = 0^\circ$). η was assumed to be zero.

TABLE 1

Quadrupole Tensor Parameters (12) and the Euler Angles Relating the PAF (Principle Axis Frame) of D(4) to the PAF of D(5)

Atom ^a	$\omega_Q/2\pi/\text{kHz}$	η	ϕ	θ	χ
D(4)	159.99	0.043	-32.1°	108.6°	44.0°
D(5)	169.41	0.085			

^a The numbering of the atoms in (13) is adopted.

glycine- d_2 , which was calculated following the procedure given by Linder *et al.* (11) and using the quadrupolar parameters listed in Table 1 (12). Due to the different quadrupolar coupling constants $\omega_Q^{(i)}$ of the two deuterons, two curves appear. Further, the nonzero asymmetry parameters η_i lead to the nondegenerated ridges nearly perpendicular to the frequency axes (2, 11). For clarity, we only show the ridges arising from one of the two transitions in the ^2H spin system. The omitted ridges in the 2D plot would give rise to mirror images with respect to the line of $f_1 + f_2 = 0$ in Fig. 3a. From this ridge plot, we can see that the linewidth of the excited line must be below about 5 kHz to separate the two ridges crossing the f_1 axis at about ± 105 kHz.

First, we made the experiment with narrowband excitation by CP-TAPF only. Its corresponding initial lineshape is given in Fig. 1c, and the resulting 1D exchange spectrum is shown in Fig. 4a. The peaks at ± 67.9 , ± 62.0 , and ± 57.1 kHz are clearly resolved and agree with the values expected from the simulation (± 69 , ± 63 , ± 58 kHz, see Fig. 3a). The expected singularities at ± 3 kHz fall on top of the excited line and are not detectable. Further, at ± 105 kHz, we found a broad peak rather than the expected two singularities, indicating that the width of the excited line is still too broad to resolve these ridges intersecting with the line $f_1 = 0$ at a flat angle. To achieve the desired spectral resolution, we added a DANTE pulse train to CP-TAPF (Fig. 1d). The corresponding 1D exchange spectrum is shown in Fig. 4b: the singularities at ± 103.0 and ± 109.9 kHz are clearly resolved and agree with the expected values of ± 105 and ± 111 kHz, respectively. The large fluctuation observed around the base of the excited line is known as DANTE wiggles.

The other observed strong lines at ± 47.9 kHz cannot be interpreted by the theoretical ridge plot (Fig. 2a) based on spin diffusion between the two deuterons within a single molecule. Hence, we attributed them to *intermolecular* transfer of polarization, i.e., spin diffusion between closely spaced molecules. We examined the distance R between a given reference deuteron and its neighbors as well as the angle θ between the unique tensor axes of the reference deuteron and its neighbors from the crystal structure of α -glycine (13). For the second-nearest pair of deuterons ($R = 0.275$ nm, $\theta = 69.6^\circ$) its ridge plot would almost be overlapped by those from the intramolecular peaks ($R = 0.176$ nm, $\theta = 108.1^\circ$) because the

experiment cannot distinguish between θ and $\pi - \theta$ ($69.6^\circ \sim 180 - 108.1^\circ$). For the third-nearest two D(4) deuterons ($R = 0.299$ nm, $\theta = 159.7^\circ$), the corresponding 2D ridge plot is shown in Fig. 2b, which indicates that the 1D exchange spectrum should exhibit two peaks at ± 46 and ± 61 kHz. In calculation, η was assumed to be zero for simplicity. The calculated peaks at ± 61 kHz coincide with the observed ones at ± 62.0 kHz belonging to intramolecular spin diffusion and are not detectable separately. The other peaks at ± 46 kHz agree with the observed ones at ± 47.9 kHz. Thus, it has been shown that the present 1D exchange experiment with a mixing time of 500 ms can successfully measure the angle between two C–D bonds with a D–D distance of at least 0.3 nm.

Single quantum polarization transfer (spin diffusion) be-

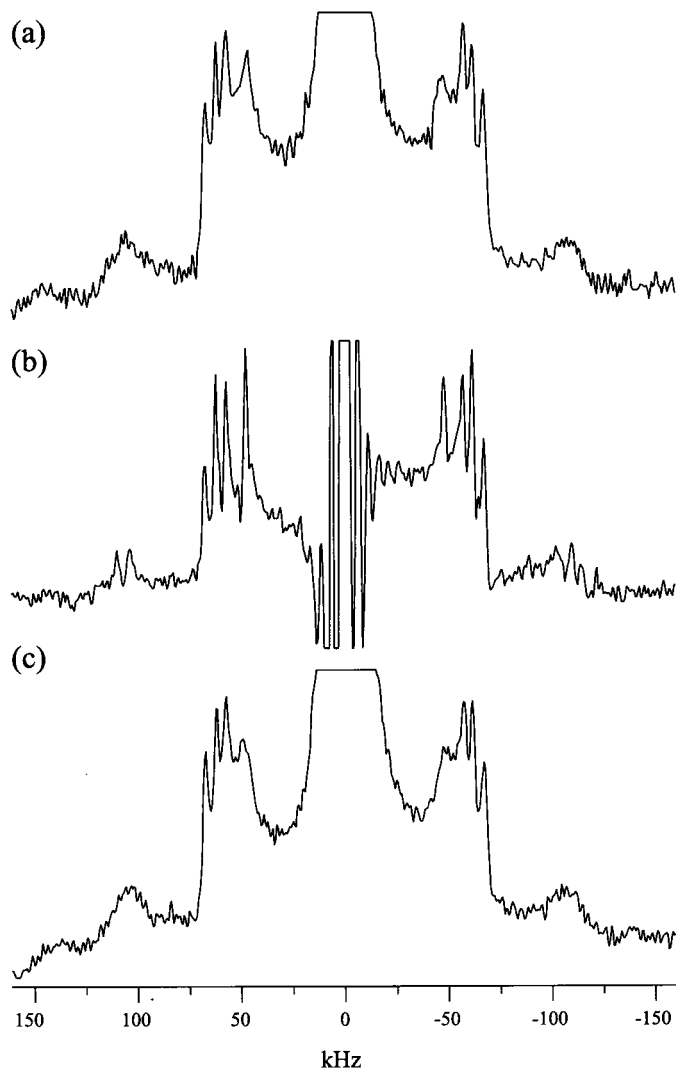


FIG. 4. 1D exchange spectra for different narrowing procedures. Experimental parameters are given in Fig. 1. (a) Narrowing by CP-TAPF; $\tau_m = 500$ ms, 70,000 accumulations. (b) Narrowing by CP-TAPF and DANTE; $\tau_m = 500$ ms, 120,000 accumulations. (c) Same as (a), but $\tau_m = 200$ ms, 60,000 accumulations.

tween two deuterons i and j with an equal sign for their quadrupolar frequencies q_i and q_j can be described mainly in terms of the diffusion rate $k_{\text{SD}} = k^{(23)} = k^{(78)}$ (14), where the superscript numbers represent the spin state as $2 = (I_z^i, I_z^j) = (1, 0)$, $3 = (0, 1)$, $7 = (0, -1)$, and $8 = (-1, 0)$. k_{SD} is given by

$$k_{\text{SD}} = 4\omega_{\text{D}_{ij}}^2 g_{ij}(q_i - q_j), \quad [1]$$

with the dipolar coupling coefficient $\omega_{\text{D}_{ij}}$ and the lineshape function of the zero-quantum transition $g_{ij}(q_i - q_j)$ evaluated at an offset $q_i - q_j$. For q_i and q_j with opposite signs, the apparent diffusion rate is governed by the transitions among the $(-1, 1)$, $(0, 0)$, and $(1, -1)$ states and is given by (14)

$$k_{\text{SD}} = 6\omega_{\text{D}_{ij}}^2 g_{ij}(q_i + q_j). \quad [2]$$

Under level crossing (matching of ^2H frequencies, $|q_i| = |q_j|$), the lineshape function $g_{ij}(q_i \pm q_j)$ may be written as

$$g_{ij}(0) \sim \frac{1}{\Delta g_i(\omega)}, \quad [3]$$

where $\Delta g_i(\omega)$ is the linewidth given by ^1H - ^2H and ^2H - ^2H dipolar couplings. A coarse estimation confirms that the level crossing takes place for a short period in the mixing time τ_m , and the effective mixing time per level crossing may be given as

$$\tau_m^{\text{eff}} \sim \frac{\Delta g_i(\omega)}{\omega_Q} \tau_m. \quad [4]$$

Therefore, $k_{\text{SD}}\tau_m^{\text{eff}}$ becomes

$$k_{\text{SD}}\tau_m^{\text{eff}} \sim \frac{a\omega_{\text{D}_{ij}}^2}{\omega_Q} \tau_m, \quad [5]$$

with $a = 4$ for Eq. [1] and $a = 6$ for Eq. [2]. By putting $\tau_m = 500$ ms, $\omega_Q = 250$ kHz, and $\omega_{\text{D}_{ij}} \sim 1$ kHz estimated for the intramolecular D–D distance of 0.176 nm, we obtain $k_{\text{SD}}\tau_m^{\text{eff}} \sim 10$ for $\tau_m = 500$ ms. Since the level crossing occurs from two to four times per π rotation (3), the exchange takes place at the full exchange limit $k_{\text{SD}}\tau_m^{\text{eff}} \gg 1$. For intermolecular deuterons with a D–D distance of 0.3 nm, $k_{\text{SD}}\tau_m^{\text{eff}} \sim 0.4$, which is passably enough to observe spin diffusion.

To confirm the above assignment for the peaks at ± 47.9 kHz, we performed an additional exchange experiment with a mixing time τ_m of 200 ms rather than 500 ms without DANTE. The number of level crossings does not change by faster turning, while the effective mixing time per crossing becomes shorter now. This must decrease the intensities of the intermolecular exchange peaks compared to the intramolecular peaks.

A 1D exchange spectrum taken at $\tau_m = 200$ ms is shown in Fig. 4c. In comparison with Fig. 4a, the peaks at ± 47.9 kHz are much less intense, thus supporting their assignment to intermolecular spin diffusion.

The narrowing effect due to the addition of a DANTE pulse train is larger in the peaks at ± 47.9 and ± 62.0 kHz than in those at ± 57.1 and ± 67.9 kHz. This can be understood as follows: the latter two intramolecular peaks come from the ridges with $df_1/df_2 \sim \infty$ at $f_1 = 0$; in the intermolecular peaks at ± 47.9 kHz, the corresponding ridge cross the f_1 axis with a small slope df_1/df_2 ; the peaks at ± 62.0 kHz are an overlap of the intermolecular ridge with a small slope and that from the intramolecular ridge with a large slope, and the former is the cause of the narrowing.

CONCLUSION

We showed that by combining single-quantum $^1\text{H} \rightarrow ^2\text{H}$ cross polarization at a low ^2H RF field and a filter sequence, one can realize narrowband excitation in a ^2H powder pattern with a bandwidth of ~ 5 kHz without losing the intensity significantly at the ^2H on-resonance frequency. We applied the narrowband excitation to reduce the dimensionality of the 2D exchange experiment for structural investigations in organic solids. It was shown that the 1D-exchange spectrum contains all the information of the corresponding 2D exchange experiment, and further information hidden in the 2D spectrum by experimental artifacts can be extracted. This allows us to determine interbond angles such as dihedral angles and relative orientations of molecules. We believe that the ideas used to perform the narrowband excitation can also be useful for other experiments, like investigation of molecular dynamics using the same 2D exchange method.

ACKNOWLEDGMENTS

One of us (D.R.) thanks the Deutsche Forschungsgemeinschaft, the Fonds der Chemischen Industrie, and Prof. H. Schneider (Halle University, Germany) for support. The project was further supported by a Grant-in-Aid for Science Research from the Ministry of Education, Science, and Culture of Japan.

REFERENCES

1. For a review, see H. W. Spiess, Deuteron NMR—A new tool for studying chain mobility and orientation in polymer, *Adv. Polymer. Sci.* **66**, 23 (1985).
2. C. Schmidt, S. Wefing, B. Blümich, and H. W. Spiess, Dynamics of molecular reorientations: direct determination of rotational angles from two-dimensional NMR of powders, *Chem. Phys. Lett.* **130**, 84 (1986); K. Schmidt-Rohr and H. W. Spiess, "Multidimensional Solid-State NMR and Polymers," Academic Press, New York (1994).
3. K. Takegoshi, M. Ito, and T. Terao, Deuteron 2D sample-turning NMR: Determination of interbond angles, *Chem. Phys. Lett.* **260**, 159 (1996).
4. B. Blümich, A. Hagemeyer, K. Schmidt-Rohr, and H. W. Spiess,

- Ultra-slow molecular motion in polymers: 1D and 2D NMR spectroscopy, *Ber. Bunsenges. Phys. Chem.* **93**, 1189 (1989).
5. D. Theimer and G. Bodenhausen, Selective inversion in inhomogeneously broadened powder spectra, *Appl. Magn. Reson.* **3**, 1071 (1992).
 6. M. J. Brown, G. L. Hoatson, and R. L. Vold, Shaped pulses for selective inversion in solid-state deuterium NMR spectroscopy, *J. Magn. Reson. A* **122**, 165 (1996).
 7. G. Bodenhausen, R. Freeman, and G. A. Morris, A simple pulse sequence for selective excitation in Fourier transform NMR, *J. Magn. Reson.* **23**, 171 (1976).
 8. P. Tekely, J. Brondeau, K. Elbayed, A. Retournard, and D. Canet, A simple pulse train, using 90° hard pulses, for selective excitation in high-resolution solid-state NMR, *J. Magn. Reson.* **80**, 509 (1988).
 9. K. Takegoshi and C. A. McDowell, Cross polarization using a time-averaged precession frequency. A simple technique to reduce radiofrequency power requirements for magnetization transfer experiments in solids, *J. Magn. Reson.* **67**, 356–361 (1986).
 10. Z. Gan, P. Robyr, and R. R. Ernst, Correlation of deuterium quadrupolar tensor orientation via spin diffusion magic-angle sample spinning, *Chem. Phys. Lett.* **283**, 262–268 (1998).
 11. M. Linder, A. Hohener, and R. R. Ernst, Orientation of tensorial interactions determined from two-dimensional NMR powder spectra, *J. Chem. Phys.* **73**, 4959 (1980).
 12. C. Mueller, W. Schajor, H. Zimmermann, and U. Haeberlen, Deuterium chemical shift and EFG tensors in α -glycine, *J. Magn. Reson.* **56**, 235 (1984).
 13. P. G. Jonsson and A. Kvick, Precise neutron diffraction structure determination of protein and nucleic acid components, III. The crystal and molecular structure of the amino acid α -glycine, *Acta Crystallogr. B* **28**, 1827 (1972); L. F. Power, K. E. Turner, and F. H. Moore, The crystal and molecular structure of α -glycine by neutron diffraction—A comparison, *Acta Crystallogr. B* **32**, 11 (1976).
 14. D. Suter and R. R. Ernst, Spin diffusion in resolved solid-state NMR spectra, *Phys. Rev. B* **32**, 5608 (1985).